JOURNAL OF GEOPHYSICAL RESEARCH, VOL. 99, NO. B12, PAGES 23,887–23,897, DECEMBER 10, 1994

Equation of state and wave propagation in hysteretic nonlinear elastic materials

K. R. McCall and R. A. Guyer[1]

Earth and Environmental Sciences Division, Los Alamos National Laboratory, Los Alamos New Mexico

Abstract. Heterogeneous materials, such as rock, have extreme nonlinear elastic behavior (the coefficient characterizing cubic anharmonicity is orders of magnitude greater than that of homogeneous materials) and striking hysteretic behavior (the stress-strain equation of state has discrete memory). A model of these materials, taking their macroscopic elastic properties to result from many mesoscopic hysteretic elastic units, is developed. The Preisach-Mayergoyz description of hysteretic systems and effective medium theory are combined to find the quasistatic stress-strain equation of state, the quasistatic modulus-stress relationship, and the dynamic modulus-stress relationship. Hysteresis with discrete memory is inherent in all three relationships. The dynamic modulus-stress relationship is characterized and used as input to the equation of motion for nonlinear elastic wave propagation. This equation of motion is examined for one-dimensional propagation using a Green function method. The out-of-phase component of the dynamic modulus due to hysteresis is found to be responsible for the generation of odd harmonics and to determine the amplitude of the nonlinear attenuation.

Introduction

The macroscopic elastic properties of highly heterogeneous materials, such as rock, are unusual and much more complex than those of the materials from which they are assembled. The velocity of sound c in Berea sandstone is changed by a factor of 2 upon raising the pressure P from 0.1 MPa to 100 MPa [*Bourbie et al.,* 1987]. A factor of 2 change in the velocity of sound in SiO_2, nominally the material from which Berea sandstone is composed, requires a pressure increase of the order of 10^4 MPa [*Ashcroft and Mermin,* 1976]. Thus equations of state for a typical rock, for example, stress versus strain, show nonlinearity that is orders of magnitude greater than that of conventional materials [*Aleshin et al.,* 1980; *Meegan et al.,* 1993]. Further, these equations of state are often hysteretic and possess memory features called discrete memory or end point memory [*Holcomb,* 1981; *Boitnott,* 1992; *Gist,* 1994].

The fundamental reason for the hysteretic nonlinear elastic behavior of rock is that rock contains an enormous variety of mesoscopic structural features (for example, cracks, joints, and contacts, of typical size $\approx 1\ \mu$m) with elastic properties that are specific to their structure. It is these mesoscopic elastic units that dominate the response of the rock to both the external pressure used to find a quasistatic equation of state and the internal pressure that accompanies an elastic wave.

The purpose of this paper is to describe a theory of the elastic behavior of hysteretic nonlinear materials. We describe both the ambient state of the rock and perturbations away from that state. In the next section, we introduce the Preisach-Mayergoyz (P-M) model of hysteretic systems [*Preisach,* 1935; *Mayergoyz,* 1985; *Macki,* 1993] and adapt it to describe the hysteretic mesoscopic elastic units (HMEU) determining the elastic properties of a rock. We combine the P-M model for the behavior of the HMEU with effective medium theory (EMT) [*Kirkpatrick,* 1971] to find the elastic response of a rock that has experienced a specified pressure history. We discuss the quasistatic stress-strain equation of state, the quasistatic modulus-stress relationship, and the dynamic modulus-stress relationship. Next, we consider elastic wave propagation in a hysteretic nonlinear elastic material governed by a history dependent equation of state. We examine one-dimensional propagation of compressional waves. The equation of motion for the longitudinal displacement field contains the hysteretic nonlinear dynamic modulus. We solve the equation of motion for the displacement field using the Green function technique developed by *McCall* [1994]. This solution lets us identify the qualitative features in harmonic generation that are signatures of nonlinearity and hysteresis. Finally, we extend the analysis to examine attenuation due to a hysteretic nonlinear dynamic modulus.

[1]Also at Department of Physics and Astronomy, University of Massachusetts, Amherst.

Paper number 94JB01941.
0148-0227/94/94JB-01941$05.00

Equation of State

We take a rock's macroscopic elasticity to result from a system of hysteretic mesoscopic elastic units (HMEU). The connection between the HMEU and an equation of state is made by combining a Preisach-Mayergoyz (P-M) description of HMEU behavior with effective medium theory (EMT). In this section, we use a simple model for the HMEU to illustrate calculation of equations of state and discuss their properties.

Model the rock by a lattice of HMEU with lattice spacing nominally 10 μm. To each HMEU we assign two sets of parameters, a pair of pressures (P_c, P_o), where $P_c \geq P_o$, and a pair of equilibrium lengths (ℓ_c, ℓ_o). The meaning of these parameters in terms of the behavior of the HMEU is illustrated in Figure 1. Assume for illustrative purposes that the structural features we are describing with the HMEU are compliant cracks. Then the subscript c stands for closed and the subscript o stands for open. As the pressure applied to the HMEU is raised from zero the HMEU responds by enforcing the equilibrium length ℓ_o. At P_c the HMEU changes behavior and responds to pressures above P_c by enforcing the equilibrium length ℓ_c. If the pressure is decreased from above P_c the HMEU enforces ℓ_c until the pressure reaches $P_o \leq P_c$, at which time it reverts to enforcing ℓ_o. Thus each HMEU has hysteretic elastic behavior as a function of pressure. Since a 1-cm^3 piece of rock contains a vast number of structural features, 10^9–10^{12}, this abstraction is justified. The equilibrium lengths (ℓ_c, ℓ_o) may have a deterministic or statistical connection to (P_c, P_o).

In Figure 2a we show pairs of (P_c, P_o) in Preisach-Mayergoyz (P-M) space. These pressure pairs were generated according to the rule described below in example 1. The density of HMEU in the space of (P_c, P_o) pairs, i.e., the number of elastic units in $dP_c dP_o$ at (P_c, P_o), is $\rho(P_c, P_o)$. A pressure protocol brings the rock from $P = 0$ to $P \neq 0$ with n pressure reversals. This history leads to a separation of P-M space into two parts bounded by the curve $E(P_c, h)$ (see Figure 2a), where h stands for the pressure history leading to the rock's current pressure state P. The pressure history of the rock and $E(P_c, h)$ depend on the points of pressure reversal $P_1, \cdots, P_n$, the maximum pressure to which the rock has been subjected $P_{\max}$, and the current pressure P. In Figure 2a the HMEU below and to the left of $E(P_c, h)$ are in their closed configuration; the HMEU above and to the right of $E(P_c, h)$ are in their open configuration. A quasistatic equation of state for the rock, e.g., a stress-strain relationship, can be found from a variety of treatments of the lattice of HMEU.

To calculate a stress-strain equation of state for a particularly simple model of the HMEU we take the same two values (ℓ_c, ℓ_o), where $\ell_c = (1 - \alpha)\ell_o$, $0 \leq \alpha < 1$, for all HMEU. Thus the rock is a binary mixture of springs, each enforcing one of two separations according to its configuration: open or closed. In all of the quantitative work below we use $\alpha = 0.1$. We treat this inhomogeneous system using effective medium theory (EMT) as illustrated in the appendix. Independent of the particular geometry chosen for the lattice of HMEU we find that the rock can be replaced by a uniform system with springs that enforce a separation $\overline{\ell}$, where $\overline{\ell}$ is the average of ℓ,

$$\begin{aligned} \overline{\ell}[E] &= \ell_o + (\ell_c - \ell_o)N_c[E], \\ \overline{\ell}[E] &= \ell_o(1 - \alpha N_c[E]), \end{aligned} \tag{1}$$

where N_c is the fraction of closed elastic units. We define the strain

$$\epsilon[E] \equiv \frac{\overline{\ell}[E] - \ell_o}{\ell_o} = -\alpha N_c. \tag{2}$$

The notation $[E]$ stands for "functional of"; $\overline{\ell}$ is a functional of the state E. In this simple model the equation of state is completely determined by $E(P_c, h)$. A second term proportional to P/K_0, where K_0 is the modulus of the individual grains, could be added to (2) to account for linear elasticity in the grains, the asymptotic response of the rock at pressures high enough to close defects but below failure. We will neglect the linear grain elasticity, since its contribution to the total strain is additive and, in most cases, small compared to the nonlinear component.

If the density in P-M space $\rho(P_c, P_o)$ is strictly diagonal,

$$\rho(P_c, P_o) = A(P_c, P_o)\overline{P}\delta(P_c - P_o), \tag{3a}$$

where $\overline{P}$ is an average pressure to normalize the delta function. The stress-strain equation of state has no hysteresis, the individual HMEU have no hysteresis, and the rock as a whole has no hysteresis. The area of a hysteresis loop is related to the fraction of the density $\rho(P_c, P_o)$ that is off the diagonal. A typical rock will have ρ of the form

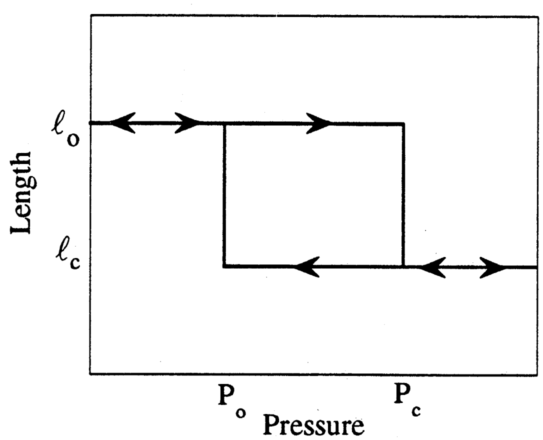

Figure 1. A hysteretic mesoscopic elastic unit (HMEU). A HMEU is characterized by a pair of pressures (P_c, P_o) and a pair of equilibrium lengths (ℓ_c, ℓ_o). At low pressure the equilibrium length of the HMEU is ℓ_o. Upon raising the pressure to P_c, the equilibrium length of the HMEU is ℓ_c. The equilibrium length remains ℓ_c until the pressure is reduced to below P_o.

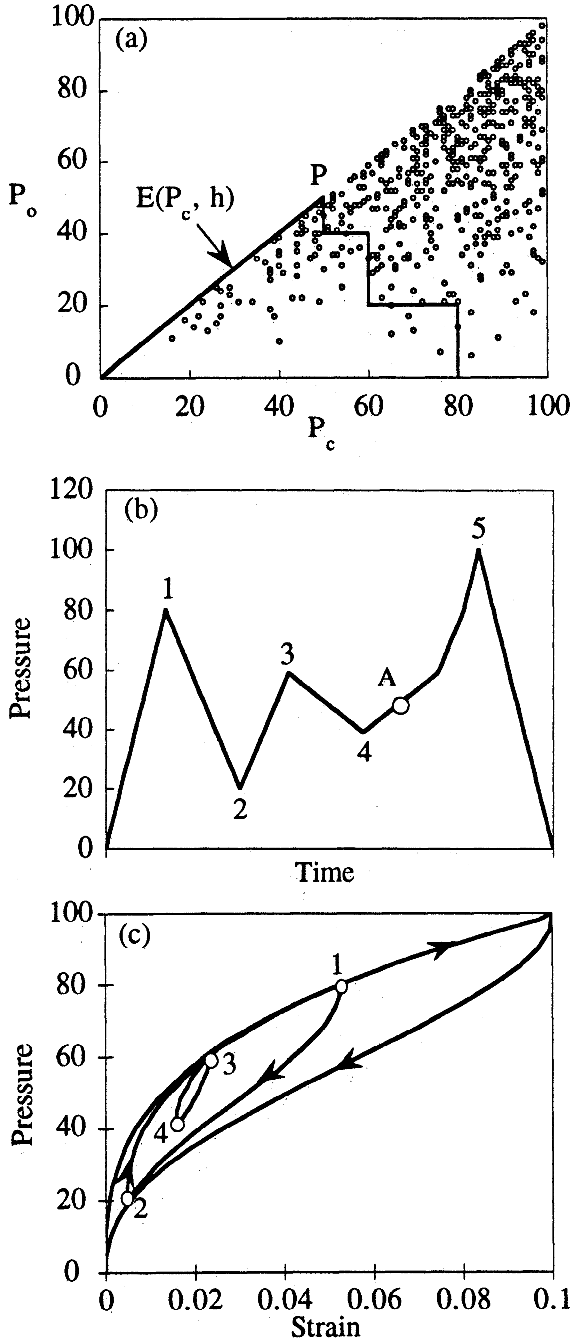

Figure 2. Elastic equation of state, example 1. (a) The points (P_c, P_o) in P-M space; 500 points generated from equation (4) are shown. The heavy curve corresponds to $E(P_c, h)$ for the pressure protocol at point A in Figure 2b. (b) The pressure history followed in constructing the equation of state. Points 1–5 are points of pressure reversal. (c) The stress-strain equation of state appropriate to Figures 2a and 2b and equation (2).

$$\rho(P_c, P_o) = A(P_c, P_o)\overline{P}\delta(P_c - P_o) + B(P_c, P_o), \quad \text{(3b)}$$

where $B(P_c, P_o)$ is the off-diagonal component of ρ. Discrete memory in the number of open or closed HMEU is a consequence of the structure of P-M space. Discrete memory in the stress-strain equation of state follows from (2).

Example 1

A set of 8000 points (P_c, P_o) in P-M space were generated according to the rule

$$\begin{aligned} P_c &= 100 r_c^{1/3}, \\ P_o &= P_c r_o^{1/3}, \end{aligned} \quad (4)$$

where r_c and r_o are random numbers uniformly distributed between 0 and 1. Representative points found from this rule are shown in Figure 2a. The rock modeled by this set of HMEU is carried through the pressure protocol shown in Figure 2b in which the pressure is raised and lowered three times. Values of the pressure are in arbitrary units. At point A on the pressure protocol the pressure history has included four points of pressure reversal, denoted 1–4. The corresponding separation curve $E(P_c, h)$ is shown in Figure 2a. As the pressure advances beyond 80, a new pressure regime is explored, and the pressure reversal points 1–4 are erased. In Figure 2c, we show stress as a function of the magnitude of strain appropriate to the P-M space in Figure 2a, the pressure history in Figure 2b, and equation (2). The hysteresis loops are traversed in the clockwise direction. The qualitative property of these hysteresis loops, that the strain does not immediately release with a decrease in pressure, results from the off-diagonal part of $\rho(P_c, P_o)$. Some of the elastic units that close upon advancing P by ΔP do not reopen upon reducing the pressure by ΔP. Discrete memory is apparent in the stress-strain curve. These stress-strain relations involve large, slow changes in pressure. Thus we refer to them as the quasistatic stress-strain equations of state.

Example 2

A set of 8000 points (P_c, P_o) in P-M space were generated according to the rule

$$\begin{aligned} P_c &= 100 r_c^2, \\ P_o &= P_c \sqrt{r_o}, \end{aligned} \quad (5)$$

where r_c and r_o are random numbers uniformly distributed between 0 and 1. Representative points found from this rule are shown in Figure 3a. The rock modeled by this set of HMEU is carried through the pressure protocol shown in Figure 3b. This pressure protocol is similar to one used by *Boitnott* [1993] in a study of hysteresis in the Young's modulus of Berea sandstone. In Figure 3c we show the stress-strain curve appropriate to the P-M space in Figure 3a, the pressure history in Figure 3b, and (2). There are qualitative differences between the stress-strain curves in Figures 2c and 3c that correlate with the P-M space densities shown in Figures 2a and 3a. The P-M space density in Figure 2a is highest at high pressures, while the P-M space density

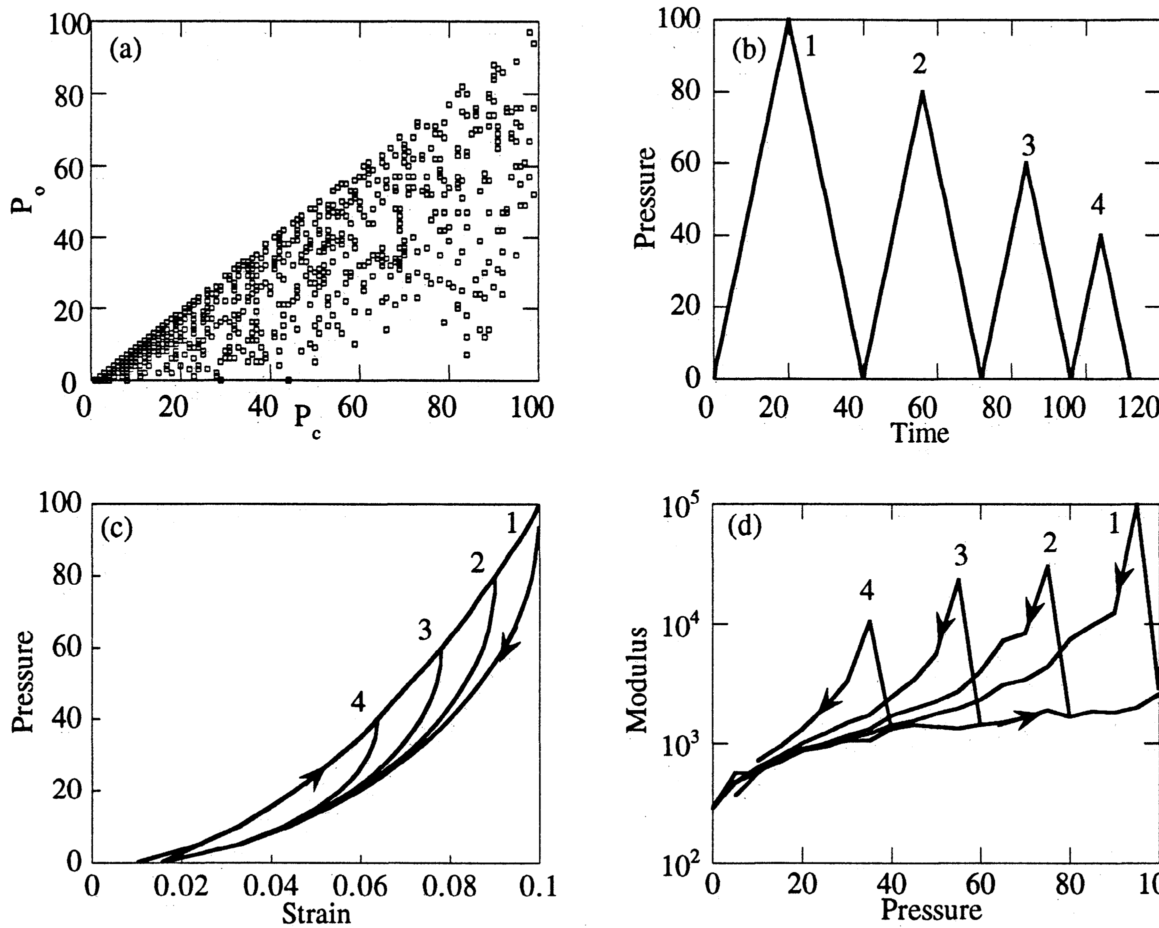

Figure 3. Elastic equation of state, example 2. (a) The points (P_c, P_o) in P-M space; 1000 points generated from equation (5) are shown. (b) The pressure protocol. (c) The stress-strain equation of state appropriate to Figures 3a and 3b and equation (2). (d) The elastic modulus as a function of stress from equation (6). The points of pressure reversal are labeled 1–4 in Figures 3b–3d.

in Figure 3a is highest at low pressures. Thus the rate of strain change with pressure is highest at high pressure in example 1 (negative curvature in the pressure versus strain curve) and highest at low pressure in example 2 (positive curvature in the pressure versus strain curve).

The elastic modulus is defined in terms of the stress-strain equation of state:

$$K = \frac{\partial \sigma}{\partial \epsilon}. \tag{6}$$

In Figure 3d, we show the modulus as a function of stress, calculated from (6) and the stress-strain equation of state in Figure 3c. The modulus-stress equation of state has a bow tie appearance (very lopsided in this example) because of the cusps at the end points of each stress-strain hysteresis loop. The modulus is discontinuous at these end points. For all four hysteresis loops in Figure 3c, the low-P part of the equations of state are the same; the HMEU opened and closed at low pressure are the same for all four loops. These qualitative features agree with the results of experimental investigations [*Boitnott,* 1992].

Example 3

P-M space was filled in the same way as in example 2 (see Figure 3a). The rock is carried through the pressure protocol shown in Figure 4a. This pressure protocol takes the rock around a large hysteresis loop with 18 small closed excursions along the way. The stress-strain curve that results from the P-M space in Figure 3a, the pressure protocol in Figure 4a, and (2) is shown in Figure 4b. Each of the small pressure excursions generates a small hysteresis loop in the interior of the large loop. If we calculate the elastic modulus around a small loop using (6), we find a bow tie shaped hysteresis loop just as for the large loops of the previous examples. As a small loop gets smaller, we may wish to study an average property of the loop. We define the average modulus of a stress-strain hysteresis loop to be the slope of the line connecting the lower cusp

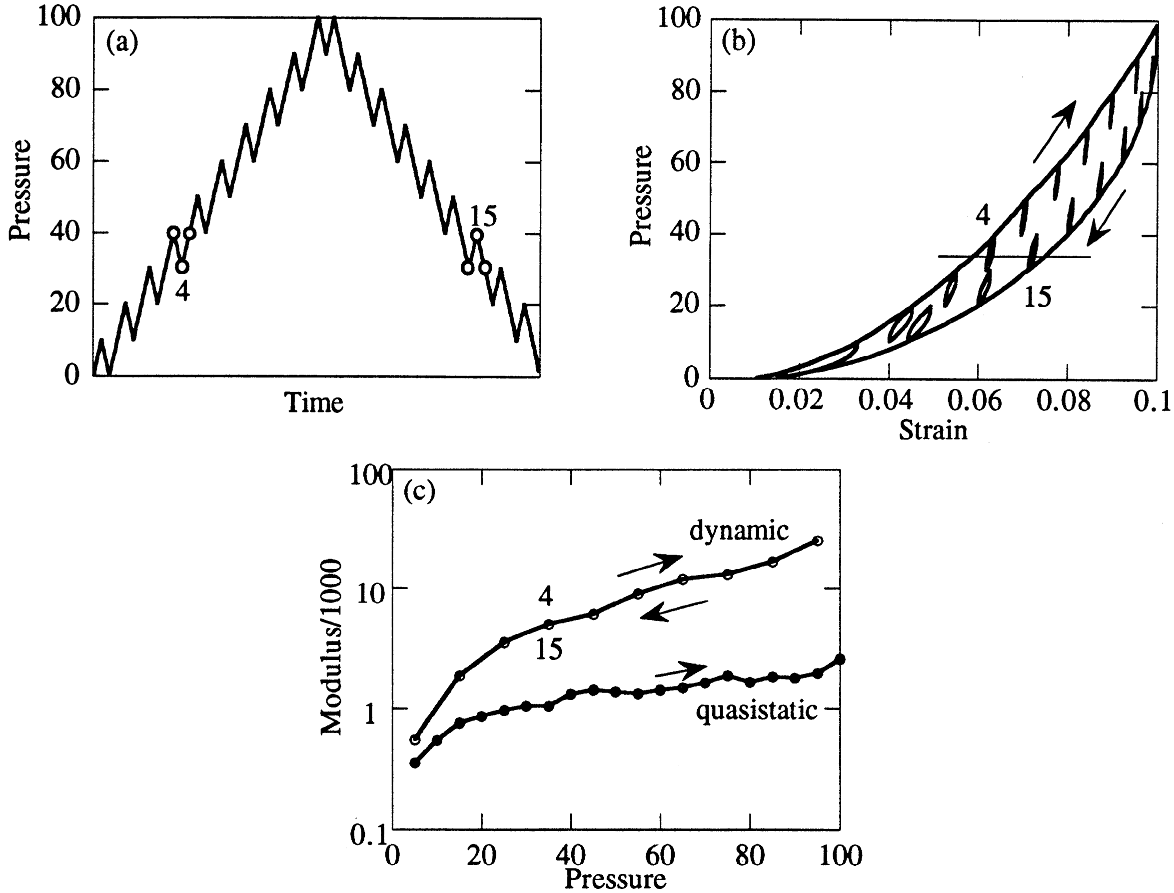

Figure 4. Elastic equation of state, example 3. The P-M space is filled as in Figure 3a. (a) The pressure protocol. The pressure goes from 0 to 100 in steps of 10 with a pressure reversal at $10, 20, \cdots, 100$. A similar procedure is followed as the pressure goes from 100 to 0. (b) The stress-strain equation of state appropriate to the P-M space of Figures 3a and 4a and equation (2). The large hysteresis loop and the small hysteresis loops are all traversed clockwise. (c) The elastic modulus of the large loop for increasing pressure (solid circles), and the average modulus as a function of stress for the interior loops labeled in Figure 4b (open circles).

to the upper cusp. Since the small loops are interior to the large loop, the average modulus must be larger for small stress-strain loops than for large stress-strain loops.

In Figure 4c we show the average modulus-stress relationship for the 17 loops labeled in Figure 4b. We imagine that the modulus appropriate to the description of wave propagation is similar to that derived from the small loops we see in Figure 4c. Thus we conclude that a modulus measured dynamically will be larger than a modulus measured quasistatically and would exhibit bow tie behavior if the entire hysteresis loop rather than its average value were studied.

Note that small stress-strain loops on opposite sides of the large stress-strain loop involving the same pressure excursion have the same average modulus, e.g., loops 4 and 15. Thus the average modulus as a function of ambient pressure has no hysteresis. The empirical fact is that both the stress-strain equation of state and the average modulus-stress relationship are hysteretic [*Gist*, 1994]. The model of elastic response of a rock that we have developed to this point gives one of these results but not the other. So far the pressure that acts on the individual HMEU is the external pressure on the system. Below we consider a simple example in which the HMEU respond to the average condition of the rock.

Example 4

A set of 8000 points (P_c, P_o) were generated according to the rule

$$\begin{aligned} P_c &= 100 r_c^2, \\ P_o &= P_c r_o^{(0.25+0.75 N_c)}, \end{aligned} \tag{7}$$

where r_c and r_o are random numbers uniformly distributed between 0 and 1. Equation (7) is equivalent to a mean field interaction between the HMEU, which makes the behavior of the individual HMEU depend on the average condition of the rock. When $N_c = 0$, the HMEU fill P-M space primarily near the diagonal. When $N_c = 1$, the HMEU fill P-M space more uniformly. In Figure 5a, the initial distribution of HMEU corresponding to $P = 0$, $N_c = 0$, is shown with solid circles; the distribution of HMEU corresponding to $P = 100$, $N_c = 1$, is shown with open squares. The rock is carried through the pressure protocol in Figure 4a. The resulting stress-strain equation of state is shown in Figure 5b. In Figure 5c, we show the quasistatic modulus-stress relationship derived from the slope of the large stress-strain hysteresis loop and the average modulus-stress relationship derived from the small stress-strain hysteresis loops. The average modulus for small pressure excursions, i.e., the equivalent of the average dynamic modulus, is always greater than the quasistatic modulus at the same pressure. The average modulus-stress relationship is hysteretic but continuous at its ends, in contrast to the quasistatic modulus-stress relationship. Both measures of modulus versus stress have end point memory.

Elastic Wave Propagation

In this section we apply a Green function formalism developed by *McCall* [1994] to describe elastic wave propagation in rock. We wish to focus on the consequences of hysteresis and will therefore limit ourselves to the propagation of compressional waves in a single dimension.

We take the equation of motion for the displacement field in a rock at pressure P to be

$$\rho\frac{\partial^2 u(x,t)}{\partial t^2} = \frac{\partial}{\partial x}\left\{\overline{K}\left[1+\alpha(x,t)\right]\frac{\partial u(x,t)}{\partial x}\right\} + S'(x,t), \tag{8}$$

where u is the x component of the displacement field, ρ is the (constant) rock density, $\overline{K}$ is the average dynamic modulus at P, α describes the departure of the modulus from $\overline{K}$ ($\int \alpha(x,t)dt = 0$ over one pressure cy-

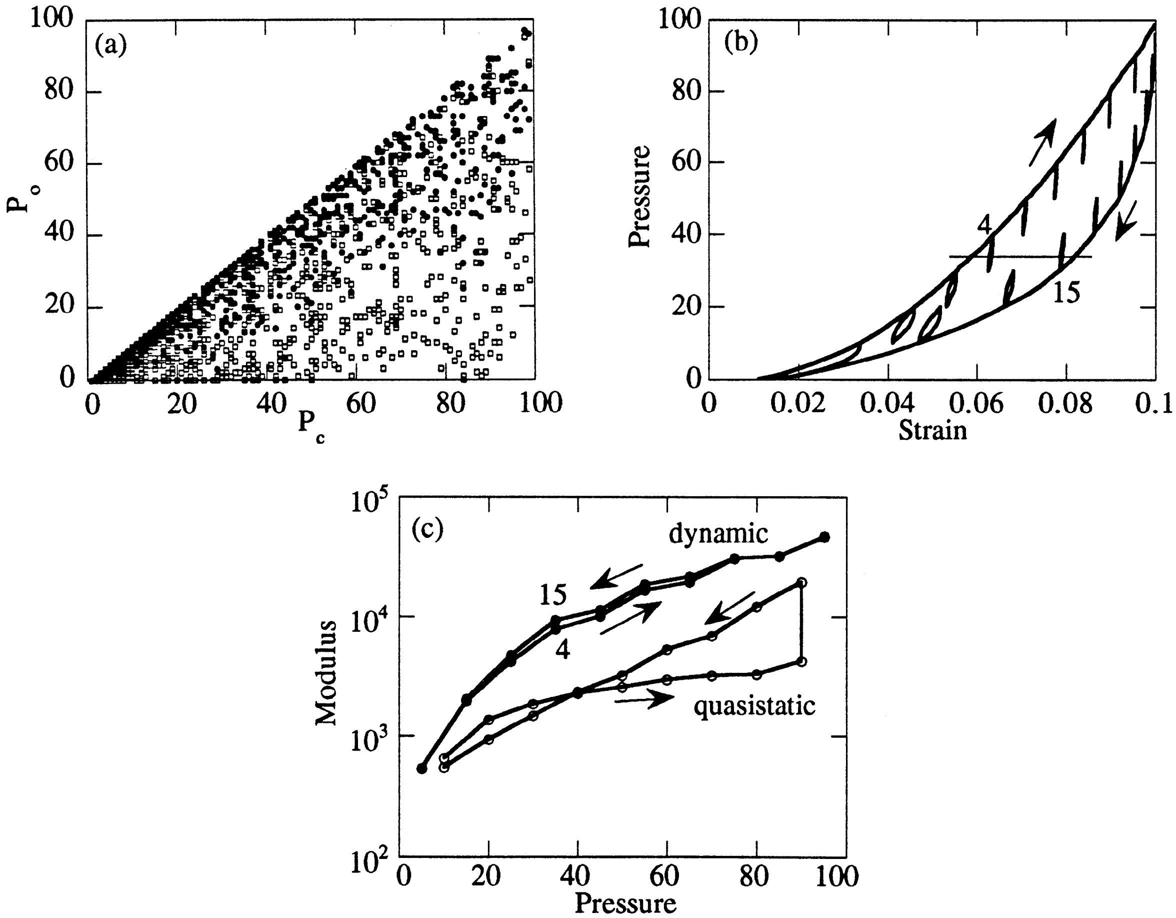

Figure 5. Elastic equation of state, example 4. (a) The points (P_c, P_o) in P-M space; 1000 points generated from (7) are shown. The solid circles are for $P = 0$, $N_c = 0$; the empty squares are for $P = 100$, $N_c = 1$. (b) The stress-strain equation of state for Figure 5a, the pressure protocol in Figure 4a, and equation (2). (c) The elastic modulus of the large loop (open circles) and the average modulus of the small loops (solid circles) as a function of stress.

cle), and $S'(x,t)$ is the external source that drives the system. The departure from constant modulus $\alpha(x,t)$ is a functional of the pressure field:

$$\alpha(x,t) = \alpha[\delta P(x,t)] = \alpha\left[\frac{\partial u(x,t)}{\partial x}\right]. \quad (9)$$

In the frequency domain, (8) becomes

$$\left(\frac{\partial^2}{\partial x^2} + k^2\right) u(x,\omega) = -S(x,\omega) - \frac{\partial}{\partial x}\int \frac{d\omega'}{2\pi}\alpha(x,\omega')\frac{\partial u(x,\phi)}{\partial x}, \quad (10)$$

where $k^2 = \omega^2\rho/\overline{K}$, $S = S'/\overline{K}$, and $\phi = \omega - \omega'$.

Using the Green function method, we develop a systematic treatment of (10) without initially specifying $\alpha(x,\omega)$ as follows.

1. Specify the external disturbance.
2. Find the Green function $g(x,x',\omega)$ for the linear problem, $\alpha(x,\omega) = 0$, and the specific geometry to be studied. This problem may include attenuation.
3. Develop $u(x,\omega)$ and $\alpha(x,\omega)$ in powers of the strength of the source $S(x,\omega)$.

Details of this procedure, such as how to include attenuation, are given by *McCall* [1994]. For the leading nonlinear correction due to $\alpha(x,\omega)$ to the linear displacement field $u_0(x,\omega)$, one finds

$$u_1(x,\omega) = \int dx' \int \frac{d\omega'}{2\pi} g(x,x',\omega)\frac{\partial}{\partial x'}\left[\alpha_0(x',\omega')\frac{\partial u_0(x',\phi)}{\partial x'}\right], \quad (11)$$

where $\alpha_0(x,\omega) = \alpha[\partial u_0(x,\omega)/\partial x]$ and the linear displacement field $u_0(x,\omega)$ is

$$u_0(x,\omega) = \int dx' g(x,x',\omega)S(x',\omega). \quad (12)$$

The traditional way of treating nonlinearity in the equation of motion of an elastic wave is to develop the strain energy as an analytic function of the strain field $\partial u/\partial x$ [*Murnaghan,* 1951; *Landau and Lifshitz,* 1959]. For hysteretic materials such as rocks, we showed that pressure cycles cause a change in the elastic modulus that is not an analytic function of $\partial u/\partial x$. Using the P-M space and EMT model, we assess the effect on the modulus of small pressure fluctuations

$$\delta P(x,t) = -\overline{K}\frac{\partial u(x,t)}{\partial x}. \quad (13)$$

For a linear displacement field $u_0 = U\sin(k_0x - \omega_0t)$ and δP_0 given by (13), we can represent $\alpha(x,t)$ in the form of a Fourier series in $\tau = k_0x - \omega_0t$:

$$\alpha_0(x,t) = \frac{a_0}{2} + \sum_{n=1}^{\infty} a_n\cos n\tau + \sum_{n=1}^{\infty} b_n \sin n\tau, \quad (14)$$

where the a_n are the amplitudes of the part of the modulus that is in phase with the pressure fluctuation and the b_n are the amplitudes of the part of the modulus that is out of phase with the pressure. The amplitudes a_n and b_n are proportional to δP_0. We have chosen $\overline{K}$ so that $a_0 = 0$.

Using the Green function for an infinite, homogeneous material, and carrying through the algebra called for by (11), we find the perturbation displacement is

$$u_1(x,t) = -\frac{k_0Ux}{2}\cos\tau\sum_{n=1}^{\infty} c_n\cos(n\tau - \phi_n), \quad (15)$$

where $c_n = (a_n^2 + b_n^2)^{1/2}$, $\tan\phi_n = b_n/a_n$, and $k_0^2 = \omega_0^2\rho/\overline{K}$.

By writing α_0 as a Fourier series in (14), we have the flexibility to look at the traditional cubic anharmonic description of nonlinearity as well as extreme cases of nonanalytic nonlinearity. However, independent of the precise nature of the nonlinear process there are several observations of general validity about $u_1(x,t)$.

1. The amplitude at distance x from the source is proportional to x, independent of the precise choice of $\alpha_0(x,t)$. This proportionality represents the fact that nonlinear elastic waves interact in the system over the entire range between source and observer.
2. The amplitude is proportional to $(k_0U)^2$. The first factor of k_0U comes from the elastic wave incident on the scattering amplitude. The second factor comes about because the amplitudes a_n and b_n are proportional to the pressure fluctuation, i.e., to k_0U.
3. Hysteresis that is responsible for the out-of-phase part of α, i.e., the b_n terms in the Fourier series, exhibits itself in the phase of the scattered wave that is seen by the observer.

Let us look at several examples to appreciate the content of (15).

Standard Cubic Anharmonicity

The traditional cubic anharmonic description of nonlinearity is equivalent to setting $\alpha = \beta\partial u/\partial x$. Thus if $u_0 = U\sin(k_0x - \omega_0t)$, then

$$\alpha_0(x,t) = \beta k_0U\cos\tau, \quad (16)$$

where $\tau = k_0x - \omega_0t$. This choice of α_0 versus δP is equivalent to setting $a_n = \beta k_0U\delta_{n,1}$ and $b_n = 0$ in (14); α_0 has a component in phase with pressure but none out of phase with pressure. The first-order nonlinear term in the displacement field, $u_1(x,t)$ in (15), is the well-known result

$$u_1(x,t) = -\frac{\beta(k_0U)^2x}{4}[\cos 2\tau + 1]. \quad (17)$$

A single-frequency source gives rise to a displacement field with a zero-frequency component and a component at twice the driving frequency, as well as the linear component at the driving frequency. The amplitude of the nonlinear term is proportional to the propagation distance x, the square of the source amplitude U, and the square of the source frequency ω_0.

Out-of-Phase Anharmonicity

Take the departure from constant modulus to be entirely out of phase with the pressure, for example,

$$\alpha_0(x,t) = \gamma k_0 U \sin 2\tau. \tag{18}$$

In this case, $a_n = 0$ and $b_n = \gamma k_0 U \delta_{n,2}$. Thus the stress-strain relationship has an in-phase part due to the average modulus $\overline{K}$ and an out-of-phase part due to the departure from constant modulus $\overline{K}\alpha_0$ (see equation (8)). The out-of-phase part of the stress with strain is the hysteresis from which attenuation is calculated. We call this choice of α_0 a hysteretic nonlinearity. For $u_1(x,t)$ we find

$$u_1(x,t) = -\frac{\gamma(k_0U)^2 x}{4}\left(\sin 3\tau + \sin\tau\right). \tag{19}$$

Note the phase difference between this result and standard cubic anharmonicity, (17). The elastic wave response to a hysteretic nonlinearity is 90° out of phase with the response to a nonhysteretic nonlinearity.

A Bow Tie

Consider the case in which the pressure has been raised monotonically to pressure $\overline{P}_+ = \overline{P} + \Delta P$ and the density in P-M space in the vicinity of $\overline{P}$ is (see equation (3b))

$$\rho(P_c, P_o) = A\overline{P}\delta(P_c - P_o) + B, \qquad \begin{array}{l} \overline{P}_- \le P_c \le \overline{P}_+ \\ \overline{P}_- \le P_o \le P_c \end{array} \tag{20}$$

where $\overline{P}_- = \overline{P} - \Delta P$, and A and B are constants. Reduce the pressure P a small amount to $\overline{P}_-$ and then raise it again, following the number closed N_c along both paths (down and up). At pressure P, where $\overline{P}_- \le P \le \overline{P}_+$, the changes in the number of closed units are

$$\Delta N_c(\downarrow) = A\overline{P}[P - \overline{P}_+] - \frac{B}{2}[P - \overline{P}_+]^2, \tag{21a}$$

$$\Delta N_c(\uparrow) = A\overline{P}[P - \overline{P}_-] + \frac{B}{2}[P - \overline{P}_-]^2. \tag{21b}$$

The corresponding strains are

$$\epsilon(\downarrow) = \epsilon(\overline{P}_+) - \alpha N_c(\downarrow), \tag{22a}$$

$$\epsilon(\uparrow) = \epsilon(\overline{P}_-) - \alpha N_c(\uparrow). \tag{22b}$$

The inverse of the modulus is given by (6):

$$\frac{1}{K} = -\frac{\partial\epsilon}{\partial P}. \tag{23}$$

For the strains of (22)

$$K(\downarrow) = \frac{\overline{K}}{1 - \lambda\,\delta p}, \tag{24a}$$

$$K(\uparrow) = \frac{\overline{K}}{1 + \lambda\,\delta p}, \tag{24b}$$

where

$$\overline{K} = \frac{1}{\alpha(A\overline{P} + B\Delta P)}, \tag{25a}$$

$$\lambda = \frac{B\overline{P}}{A\overline{P} + B\Delta P}, \tag{25b}$$

$$\delta p = \frac{P - \overline{P}}{\overline{P}}. \tag{25c}$$

For wave propagation, we take $\delta p \ll 1$ and find

$$K(\downarrow) \approx \overline{K}[1 + \lambda\delta p], \tag{26a}$$

$$K(\uparrow) \approx \overline{K}[1 - \lambda\delta p]. \tag{26b}$$

The modulus as a function of pressure looks like a bow tie.

Using the same linear displacement as in the previous examples, we set

$$\delta p(\tau) = \frac{\Delta P}{\overline{P}}\cos\tau, \tag{27}$$

and find

$$\alpha_0(x,t) = \lambda\frac{\Delta P}{\overline{P}}\begin{cases} \cos\tau, & 0 \le \tau \le \pi, \\ -\cos\tau, & \pi \le \tau \le 2\pi, \end{cases} \tag{28}$$

Because of the odd symmetry about $\tau = \pi$, the only nonzero coefficients in the Fourier series expansion of α_0, (14), are the out-of-phase with pressure coefficients b_n for n even. Equation (28) can be represented by

$$\alpha_0(x,t) = \frac{8\lambda\Delta P}{\pi\overline{P}}\sum_{n=1}^{\infty}\frac{n}{4n^2 - 1}\sin 2n\tau. \tag{29}$$

Note that the coefficients of $\sin 2n\tau$ decrease as $1/n$; thus this bow tie example is similar to the out-of-phase anharmonic example above, in leading approximation. For $u_1(x,t)$ we find

$$u_1(x,t) = -\frac{2k_0 U x\lambda\Delta P}{\pi\overline{P}} \sum_{n=1}^{\infty}\frac{n}{4n^2 - 1}\left[\sin(2n+1)\tau + \sin(2n-1)\tau\right]. \tag{30}$$

The bow tie character of the modulus is out of phase with the pressure and leads to odd harmonics in the displacement. In reality, we expect both even and odd harmonics in the displacement, with odd harmonics dominating when hysteresis is important.

A Hysteretic Modulus From Figure 5b

In Table 1 we show the amplitudes a_n, b_n, c_n, and ϕ_n of the Fourier representation, (14), of the loop 4 modulus in Figure 5b. We took the modulus loop to be

Table 1. Fourier Coefficients for a Modulus Bow Tie

n	a_n	b_n	c_n	ϕ_n
0	1.000	0.000	1.000	0.0
1	-0.107	0.050	0.118	-24.9
2	-0.066	0.326	0.333	-78.6
3	0.045	0.192	0.197	77.0
4	-0.177	0.213	0.277	-50.3
5	0.010	0.166	0.166	86.6
6	-0.143	0.158	0.213	-47.9
7	0.060	0.131	0.144	65.4
8	-0.177	0.123	0.216	-34.8
9	-0.067	0.108	0.127	58.3
10	-0.114	0.108	0.157	-43.5

the result of one cycle in pressure of an elastic wave, plotted modulus versus time, and Fourier analyzed the result. The even amplitudes of the modulus are larger than the odd amplitudes ($c_{2n} > c_{2n-1}$); the even out-of-phase amplitudes b_n are generally larger than the even in-phase amplitudes a_n (ϕ_n is large). Thus, similar to the analytic bow tie example above, the nonlinear displacement u_1 will contain strong odd harmonics and large components 90° out of phase with traditional cubic anharmonicity. From the amplitudes c_n and phase angles ϕ_n we can construct $u_1(x,t)$ according to (15).

Energy Loss; Q

In the previous section, we describe elastic wave propagation in a hysteretic, nonlinear elastic system brought to an elastic state by a prescribed pressure protocol. An important element in the calculation was the hysteretic component of the elastic response, that is, the component of $\alpha(x,t)$ in (8) that is out of phase with the pressure. This part of $\alpha(x,t)$ is described by the b_n terms in (14) and contributes to the attenuation. We define Q by

$$\frac{1}{Q} = \frac{\Delta E}{\overline{E}}, \tag{31}$$

where ΔE is the energy loss per cycle and $\overline{E}$ is the average energy in the wave during a cycle. For ΔE we take

$$\Delta E = \oint \sigma d\epsilon, \tag{32}$$

where $\oint$ stands for integration over one cycle in time, and σ is the effective stress found from the first term on the right-hand side of (8),

$$\sigma = \overline{K}\left[1 + \alpha(x,t)\right]\frac{\partial u}{\partial x}. \tag{33}$$

We develop ΔE as a series in the strength of the nonlinearity in direct analogy with the method of solution to (8) in *McCall* [1994]. We find to first order that $\Delta E = \Delta E_0 + \Delta E_1$, where ΔE_0 is the contribution to the energy loss due to the linear elastic response of the system and

$$\Delta E_1 = c_0^2 \oint \alpha(x,t)\frac{\partial u_0}{\partial x}\frac{\partial \dot{u}_0}{\partial x}dt, \tag{34}$$

where $c_0^2 = \overline{K}/\rho_0$. Using $u_0 = U\sin\tau$, where $\tau = k_0 x - \omega_0 t$, we have

$$\frac{\partial u_0}{\partial x}\frac{\partial \dot{u}_0}{\partial x} = \frac{1}{2}\omega_0 (k_0 U)^2 \sin 2\tau. \tag{35}$$

The integral around a cycle in time picks out the term in $\alpha(x,t)$ that is proportional to $\sin 2\tau$. Thus it is the amplitude b_2 of the out-of-phase component of the nonlinear elasticity that is responsible for the attenuation. We have

$$\frac{1}{Q} - \frac{1}{Q_0} \propto b_2. \tag{36}$$

where $Q_0^{-1} = \Delta E_0/\overline{E}$ and $\overline{E} = \rho c_0^2 (k_0 U)^2$.

Recall that $b_2 \propto \delta P_0 \propto k_0 U$. The hysteretic part of the nonlinear elasticity is responsible for the nonlinear attenuation. The coefficient b_2 is a measure of the size of this nonlinear attenuation [*Day et al.,* 1993]. In the work of *Day and Minster* [1984], nonlinear attenuation Q is found to be the cause of hysteresis. Here, in contrast, we find hysteresis to be the cause of nonlinear attenuation.

Conclusions

In this paper we have sketched a theoretical description of elastic behavior in hysteretic nonlinear material. We modeled the elastic material, rock, by assuming its macroscopic properties are due to a large number of hysteretic mesoscopic elastic units (HMEU). To obtain the elastic equations of state, we combined the Preisach-Mayergoyz (P-M) description of a set of HMEU with effective medium theory (EMT). This treatment emphasizes the importance of pressure history in the determination of the elastic state of a rock. The connection between the density of HMEU in P-M space $\rho(P_c, P_o)$ and qualitative features of the stress-strain equation of state, the quasistatic modulus-stress relationship, and the dynamic modulus-stress relationship were illustrated with four examples.

The qualitative features seen in the quasi-static modulus-stress relationship are also present in the small-amplitude pressure cycles that accompany propagation of an elastic wave. Thus a hysteretic nonlinear dynamic modulus is input to the description of elastic wave propagation in a rock. We employed a Green function method to study the equation of motion of the longitudinal displacement field in the presence of such a modulus. This method let us develop a systematic hierarchy of equations for the displacement field. We described the behavior of the displacement field for a series of examples. Finally, we described the connection between hysteretic nonlinear elasticity and the nonlinear attenuation.

This theoretical description of elastic behavior in hysteretic nonlinear elastic material gives us most rock properties, independent of a particular model of mesoscopic structural features: (1) a hysteretic quasi-static stress-strain equation of state with end point memory, (2) a quasi-static modulus-stress relationship in the form of a bow tie, (3) a hysteretic dynamic modulus-stress relationship with end point memory, (4) a dynamic modulus greater than the corresponding quasistatic modulus, (5) a description of elastic wave propagation, using the dynamic modulus-stress relationship, that leads to copious production of odd harmonics, and (6) a connection between the strength of the nonlinear attenuation and the strength of odd harmonic production.

We close this section with a series of remarks about the theoretical model. First, we have found items 1–5 above by forward modeling. The P-M space description of the HMEU may be used in conjunction with experimental measurements to do the inverse problem and learn about the structural features in a rock (work in progress). Second, among the issues that must be considered when comparing measurements to the theoretical model are (1) are effective medium theory and mean field theory adequate, and (2) what model of the HMEU is most appropriate? Third, we have only touched on the relationship between Q and nonlinear attenuation. We plan to return to this phenomenon in the context of specific HMEU models in the immediate future. Fourth, we have discussed the equations of state using a particularly simple abstraction of the properties of the structural features. More elaborate modeling is possible and tractable. That such a treatment will work is clear from the series of papers by *Holcomb* [1981] in which a description qualitatively equivalent to the P-M space description is validated. Fifth, the elastic state of a rock is not solely determined by its pressure history. The behavior of the HMEU is strongly influenced by the fluid saturation history of the sample. Filling and emptying fluid from a pore system is itself a history dependent phenomena that can be described using the P-M space picture [*Smith et al.*, 1987; *Guyer*, 1993]. (6) For a pressure fluctuation associated with an acoustic disturbance, the timescale is 10^{-2}–10^{-6} s. For a pressure fluctuation associated with a quasi-static measurement [*Boitnott*, 1992; *Gist*, 1994], the timescale is 1–10 s. The hysteretic response of a system may well depend on timescale [*Brennan*, 1981]. We have made no attempt to add this frequency dependence to our model. It is straightforward, however, to model a system of HMEU with frequency dependent response, and the P-M space description lends itself naturally to this.

Our treatment of the elastic equation of state and of elastic wave propagation have general validity. However, we have deliberately used a sequence of approximations that lets us show the content of the model with a minimum of computational complexity. These approximations and simplifications are not required; we can move away from them when our understanding of the mesoscopic structure of the system becomes firmer or when we adopt specific models of the HMEU.

Appendix: Effective Medium Theory

The goal of effective medium theory is to replace a nonuniform system by a uniform system with an average property characteristic of the nonuniform system. The method is to embed a single unit with the distribution of characteristics in the original system in an otherwise uniform system, average over the distribution carried by the single unit, and require that the uniform system have a value that makes the average over the single unit vanish.

Model a system of elastic units as a lattice of masses connected by springs. For simplicity, consider a one-dimensional lattice of masses at positions $u_n = n\ell + x_n$, where ℓ is an average equilibrium length of the springs, x_n is the departure from an average equilibrium position, and $-N \leq n \leq N$. The spring between masses n and $n+1$ is characterized by an equilibrium length ℓ_{nn+1} and a spring constant Γ. Assume the motion of each mass is influenced only by its nearest neighbors. Then the potential energy of elastic unit n is

$$V_n = \frac{\Gamma}{2}\left\{[x_{n+1} - x_n + (\ell - \ell_{nn+1})]^2 + [x_n - x_{n-1} + (\ell - \ell_{nn-1})]^2\right\}, \quad \text{(A1)}$$

and the equation of motion for the position of the nth mass away from its equilibrium position is

$$m\frac{\partial^2 x_n}{\partial t^2} = \Gamma[x_{n+1} - 2x_n + x_{n-1} - (\ell_{nn+1} - \ell_{nn-1})]. \quad \text{(A2)}$$

Choose the equilibrium length enforced by the springs $\ell_{nk} = \ell$ for all springs except the spring between masses 0 and 1; let $\ell_{01} = a$. Then we rewrite (A2) as

$$m\frac{\partial^2 x_n}{\partial t^2} = \Gamma[x_{n+1} - 2x_n + x_{n-1} - (\ell - a)(\delta_{n1} - \delta_{n0})]. \quad \text{(A3)}$$

The effective medium theory requirement is that when x_n is averaged over the distribution of a, $\langle x_n \rangle = 0$. Thus we must solve for x_n. Taking the Laplace transform of (A3), specifying the $t = 0$ displacement and velocity to be zero,

$$ms^2\hat{x}_n = \Gamma[\hat{x}_{n+1} - 2\hat{x}_n + \hat{x}_{n-1} - s^{-1}(\ell - a)(\delta_{n1} - \delta_{n0})], \quad \text{(A4)}$$

where $\hat{x}_n$ is the Laplace transform of x_n. Finally, we write $\hat{x}_n$ and δ_{nm} as Fourier series in wave vector space,

$$\hat{x}_n = \frac{1}{N}\sum_q x_q e^{iq\ell n}, \quad \text{(A5a)}$$

$$\delta_{nm} = \frac{1}{N}\sum_q e^{iq\ell(n-m)}, \quad \text{(A5b)}$$

and find

$$x_q = \frac{\Gamma(\ell - a)(1 - e^{iq\ell})}{ms^3 + 4s\Gamma\sin^2(q\ell/2)}. \quad \text{(A6)}$$

Requiring $\langle x_q \rangle = 0$ leads to the result $\ell = \langle a \rangle$ used to calculate strain. This result is independent of the precise geometry of the uniform system in which the spring of length a is embedded.

Acknowledgments. We wish to acknowledge helpful discussions with J. A. Krumhansl, R. J. O'Connell, G. N. Boitnott, P. A. Johnson, and T. J. Shankland. J. R. Kamm made valuable comments on the manuscript. This research is supported by the Office of Basic Energy Science, Engineering and Geoscience under contract W7405-ENG-36; the U.S. Department of Energy, Office of Arms Control and Nonproliferation under contract ST604; and the Institute for Geophysics and Planetary Physics at Los Alamos National Laboratory.

References

Aleshin, A. S., V. V. Guchin, M. M. Krekov, A. V. Nikolaev, A. S. Sokolov, and J. M. Shalshov, Experimental investigation of nonlinear seismic waves, *Sov. Phys. Dokl.*, Engl. Transl., 260, 574, 1980.

Ashcroft, N. W., and N. D. Mermin, *Solid State Physics*, Holt, Rinehart, and Winston, New York, 1976.

Boitnott, G. N., The role of rock joints in non-linear attenuation in moderate strain amplitude regimes, semiannual report, Phillips Lab., Kirtland Air Force Base, Albuquerque, NM, August 1992.

Boitnott, G. N., Fundamental observations concerning hysteresis in the deformation of intact and jointed rock with applications to nonlinear attenuation in the near source region, in Proceedings of the Numerical Modeling for Underground Nuclear Test Monitoring Symposium, *Los Alamos Natl. Lab. Rep., LA-UR-93-3839*, 121, 1993.

Bourbie, T., O. Coussy, and B. E. Zinszner, *Acoustics of Porous Media*, Gulf, Houston, 1987.

Brennan, B. J., Linear viscoelastic behavior in rocks, in *Anelasticity in the Earth, Geodyn. Ser.*, vol. 4, edited by F. D. Stacey, M. S. Paterson, and A. Nicholas, p. 13, AGU, Washington, D.C., 1981.

Day, S. M., and J. B. Minster, Numerical simulation of attenuated wavefields using a Pade approximant method, *Geophys. J. R. Astron. Soc., 78*, 105, 1984.

Day, S. M., J. B. Minster, M. Tryon, and L. Yu, Nonlinear hysteresis in an endochronic solid, in Proceedings of the Numerical Modeling for Underground Nuclear Test Monitoring Symposium, *Los Alamos Natl. Lab. Rep., LA-UR-93-3839*, 135, 1993.

Gist, G. A., Fluid effects on velocity and attenuation in sandstones, *J. Acoust. Soc. Am., 96*, 1158, 1994.

Guyer, R. A., Magnetization isotherms and pore space geometry, *Phys. Rev. B, 48*, 3683, 1993.

Holcomb, D. J., Memory, relaxation, and microfracturing in dilatant rock, *J. Geophys. Res., 86*, 6235, 1981.

Kirkpatrick, S., Classical transport in disordered media: Scaling and effective-medium theories, *Phys. Rev. Lett., 27*, 1722, 1971.

Landau, L. D., and E. M. Lifshitz, *Theory of Elasticity*, Pergamon, New York, 1959.

Macki, J. W., P. Nistri, and P. Zecca, Mathematical models of hysteresis, *SIAM Rev., 35*, 94, 1993.

Mayergoyz, J. D., Hysteresis models from the mathematical and control theory points of view, *J. Appl. Phys., 57*, 3803, 1985.

McCall, K. R., Theoretical study of nonlinear elastic wave propagation, *J. Geophys. Res., 99*, 2591, 1994.

Meegan, G. D., Jr., P. A. Johnson, R. A. Guyer, and K. R. McCall, Observations of nonlinear elastic wave behavior in sandstone, *J. Acoust. Soc. Am., 94*, 3387, 1993.

Murnaghan, F. D., *Finite Deformation of an Elastic Solid*, John Wiley, New York, 1951.

Preisach, F., Über die magnetische Nachwirkung, *Z. Phys., 94*, 277, 1935.

Smith, D. T., K. M. Godshalk, and R. B. Hallock, Adsorption and capillary condensation of 4He on nuclepore, *Phys. Rev. B, 36*, 202, 1987.

R. A. Guyer, Department of Physics and Astronomy, University of Massachusetts, Amherst, MA 01003. (e-mail: rag@cmp.phast.umass.edu)

K. R. McCall, Earth and Environmental Sciences Division, Mail Stop F665, Los Alamos National Laboratory, Los Alamos, NM 87545. (e-mail: mccall@lanl.gov)

(Received January 7, 1994; revised July 21, 1994; accepted July 27, 1994.)